

A Decoupled Controller for Fuel Cell Hybrid Electric Power Split

Domenico Di Domenico and Giovanni Fiengo

Abstract—The power management of an hybrid system composed of a fuel cell, a battery and a DC/DC power converter is developed. A decoupled control strategy is proposed, aimed at balancing the power flow between the stack and the battery and avoiding electrochemical damage due to low oxygen concentration in the fuel cell cathode. The controller is composed of two components. The first controller regulates the compressor, and as consequence the oxygen supplied to the cathode, via a classic Proportional-Integral controller. The second controller optimally manages the current demanded by the fuel cell and battery via linear-quadratic control strategy acting on the converter.

The closed loop performance has been tested both in simulation and in real-time simulation using dSpace equipments.

Keywords: Fuel cell, hybrid system, power management, optimal control, Hardware-in-the-Loop.

I. INTRODUCTION

Fuel cells are generally considered promising alternative energy conversion systems, thanks to their very high efficiency in converting the chemical energy into electrical energy [5], [12], [16], and the zero near emissions production [4], [10]. In the future, it is possible to imagine that hydrogen could replace hydrocarbons as fuel in the vehicle transportation and in the electric energy generation.

Unfortunately, the hydrogen is not to be found directly in nature, and it needs to be produced. Several techniques are proposed for the hydrogen-generation propose [5], [13]. As an example, using the reforming principles, the petroleum by-products or the methane may be used to get hydrogen, which could be distributed and used as absolutely clean energy supply. Although the reforming process produces carbon dioxide, which is the principal cause of greenhouse effect, its production can be strictly controlled and it could be not dispersed in the atmosphere. Another way to produce hydrogen is the water electrolysis, utilizing alternative and renewable energy sources (i.e. nuclear energy, solar or aeolian energy).

Apart from the hydrogen generation, challenging issues in hydrogen storage and transportation need to be resolved. Despite all these challenges the promise for clean and efficient use of hydrogen still warrants more research and development in fuel cell automation optimizations. One of the key features of the control system devoted to the management of the fuel cell is the supply of oxygen to the cathode [15], [16], which is particularly difficult task during the high frequency transient in power demand. When

current is drawn from a fuel cell, the air supply system should replace the reacted oxygen, otherwise the cathode will suffer from oxygen starvation which damages the stack and limits the power response. In high pressure fuel cell, a compressor motor is used to provide the required air into the cathode through a manifold [11], [16].

To avoid starvation and simultaneously provide the power request, i.e. current demand, it is convenient to add a rechargeable auxiliary power source which can respond quickly to the increase in current demand.

A battery or a ultracapacitor should be an appropriate extra-power source. Both battery and ultracapacitor also appear capable to guarantee good vehicle performance and good fuel economy. In this paper, we choose a Fuel Cell Hybrid Power System (FCHPS) composed of fuel cell and battery.

Furthermore, a DC/DC power converter is placed between them (see Figure 1) to optimize the power flow between the fuel cell and the battery in order to satisfy the load power requirements while ensuring the operation within any limitations of the electrochemical components such as battery over-charge/over-discharge and fuel cell current limit [8].

In literature, several configurations of hybrid fuel cell systems are proposed [5], [6], [7], [8], [9], [16]. In particular, in [16] a model predictive control of a fuel cell and a small capacitor hybrid system is proposed to avoid oxygen starvation. In [14] a load following fuel cell system equipped with a compressor and a DC/DC converter is analyzed and model based techniques to tune two separate controllers for the compressor and the converter are shown. In [5], [8], [9] a hybrid system fuel cell-battery is proposed. Different control techniques are illustrated depending on the specific aim, i.e. to minimize the hydrogen consumption [5] or to preserve the

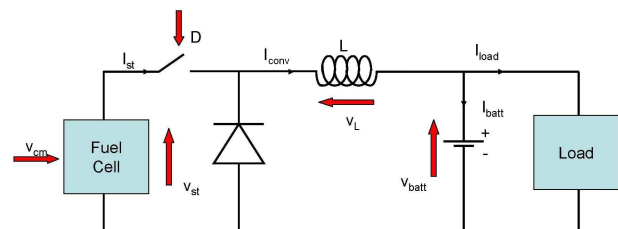


Fig. 1. Fuel Cell Hybrid Power System. v_{cm} is the compressor voltage; v_{st} and I_{st} are the voltage and current fuel cell; D is the converter duty cycle; I_{conv} is the converter current; v_L is the inductance voltage; v_{batt} and I_{batt} are the voltage and current battery; I_{load} is the current requested by the load.

This work was not supported by any organization

Domenico Di Domenico and Giovanni Fiengo are with Dipartimento di Ingegneria, Università degli Studi del Sannio, Piazza Roma 21, 82100 Benevento, Italy. E-mail: {domenico.didomenico, gifiengo}@unisannio.it

battery state of charge and to limit the stack overpotential and voltage drops [8], [9].

In the following we propose a decoupled control strategy aimed at balancing the power flow between the stack and the battery, avoiding electrochemical damage of the fuel cell. In particular, we regulate the input to the motor that drives the fuel cell air flow compressor, and as consequence the oxygen supplied to the cathode, via a classic Proportional Integral (PI) controller. We then optimally manage the current demanded to the fuel cell and battery via Linear Quadratic (LQ) control strategy acting on the converter.

In the paper, we first describe the model used for the simulations and the controllers design. We then illustrate the adopted control strategy. Software-in-the-Loop (SIL) and Hardware-in-the-Loop (HIL) simulation results and some conclusions end the paper.

II. THE MODEL

In the following the models we used to describe and test the proposed control architecture are described. We want to highlight that the fuel cell and the battery models are taken from the recent literature and our contribution is to model how these systems are connected and mainly the adopted control strategy aimed at the power management of the whole system.

A. Fuel cell

Thanks to its high power density, solid electrolyte, low corrosion and long stack life, the most promising and developed fuel cell technologies for automotive applications is the Proton Exchange Membrane (PEM) fuel cell [10], [12], [13]. In literature several PEM fuel cell models are proposed, each aimed at modeling a particular aspects based on the specific goal. As an example, a static model is proposed in [6] where the steady-state behavior of the fuel cell is described via a characteristic curve of cell voltage function of the current density. In our work, to correctly analyze the transient we used a complete fuel cell reactant model introduced by Pukrushpan, Peng and Stefanopoulou in [10]. The dynamic equations are modeled via high non linear function of the state, the compressor voltage v_{cm} and the fuel cell current I_{st}

$$\dot{x}_{fc} = f_{fc}(x_{fc}, v_{cm}, I_{st}) \quad (1)$$

This is a 9th order model, whose state variables are

$$x_{fc} = [m_{O_2} \ m_{H_2} \ m_{N_2} \ \omega_{cp} \ \dots \ \dots p_{sm} \ m_{sm} \ m_{w,an} \ m_{w,ca} \ p_{rm}]^T \quad (2)$$

where: m_{O_2} , m_{N_2} and m_{H_2} are respectively the cathode oxygen and nitrogen mass and the anode hydrogen mass; ω_{cp} is the compressor speed; p_{sm} and m_{sm} are the pressure and the inlet air mass in the supply manifold; $m_{w,an}$ and $m_{w,ca}$ are the anode and cathode water mass; p_{rm} is the return manifold pressure. For details on the non linear equations and the constant parameter values see [11], [10]. The model parameters were adjusted to assure a maximum

power generation of 75 kW, with a nominal stack voltage of 300 V and a nominal current of 250 A.

Starting from compressor voltage and stack current, the model computes the fuel cell voltage reproducing analytically the air and the hydrogen flows through the fuel cell system components. The compressor, supply manifold, cooler and humidifier are modeled for the air flow path. The hydrogen reaches the stack through its humidifier. The voltage is calculated as a function of stack current, cathode pressure, reactant partial pressures, temperature and membrane humidity. Its open circuit value is calculated from the energy balance between chemical reactant energy and electrical energy, considering the activation, ohmic and concentration losses.

The model outputs are the stack voltage v_{st} and the compressor air flow rate W_{cp} . At steady-state, the compressor air-flow needs to satisfy the desired oxygen excess ratio, λ_{O_2} , based on the following relation:

$$W_{cp} = \frac{nM_{O_2}}{4F} \frac{1 + \omega_{atm}}{x_{O_2,atm}} \lambda_{O_2} I_{st} \quad (3)$$

where n is the number of the stack elementary cells, M_{O_2} the oxygen molar mass, F the Faraday's constant, ω_{atm} the humidity ratio and $x_{O_2,atm}$ is the oxygen molar fraction in the atmospheric air drawn in the fuel cell.

B. Battery

Many battery models with different complexity exist in literature. Often a simple model with specific electrical resistor and capacitor to reproduce the electrical properties of the battery connection is used [4], [8]. Sometimes more complex models, i.e. obtained by modeling the kinetic of reactions and the diffusion phenomena [3] are presented.

In our work, we adopted a simple model [6] according to the purpose of the paper. This model describes the variation of the State Of Charge (*SOC*) of the battery as a function of the demanded current I_{batt} . In particular, the charge stored or released by the battery is computed simply by integrating the battery current. Hence the input of the model is the current, the state is the *SOC*, whose derivative is computed by dividing the incoming current by the battery capacity Q_{max} , as follows

$$\dot{SOC} = \frac{I_{batt}}{Q_{max}} \quad (4)$$

The output is the voltage v_{batt} , determined by a non-linear experimental static curve function of *SOC*.

Finally, in order to maintain the hybridization degree (*HD*), i.e. the ratio among the nominal power generated by the two sources [4]

$$HD = \frac{P_{batt}}{P_{batt} + P_{fc}} \quad (5)$$

to be equal to 0.5, the battery nominal capacity was chosen equal to 42 Ah.

C. DC-DC converter

The fuel cell and the battery model are coupled via a DC/DC converter which manages the current from the stack and the battery. Typically a DC/DC converter is a device that accepts a DC input voltage and produces a lower or higher DC output voltage.

Here, in the proposed FCHPS, the standard electric configuration of the converter is modified after substituting the capacitor of the DC/DC converter with the battery. The inputs are now the stack and the battery voltages and the outputs are the stack and the battery currents. The controller acts on the interrupt (see Figure 1), regulating the average value of the fraction of time that the converter is conducting, i.e. the interrupt is switched on. This average value is generally indicated as the duty cycle D [14], and it is considered as the control input to the system. When the controller drives the interrupt in the state ON, the fuel cell is connected to the load and provides power both to the battery and the load. Conversely, if the interrupt is OFF, the demanded power is provided exclusively by the battery. So, acting on the duty cycle it is possible to determine the average distribution of the power load between the two energy sources balancing the load current on battery and stack.

Now, considering as other inputs to the DC/DC the requested load power P_{load} , the dynamic model can be obtained according to

$$\dot{I}_{conv} = \frac{1}{L}(Dv_{st} - v_{batt}), \quad (6)$$

where the state I_{conv} is the converter current. Finally, the converter outputs are the currents towards the fuel cell and the battery, as follows

$$I_{st} = DI_{conv} \quad (7)$$

$$I_{batt} = I_{conv} - \frac{P_{load}}{v_{batt}}. \quad (8)$$

III. THE CONTROL STRATEGY

The control objective is to provide the requested power to the load while regulating the battery state of charge and the oxygen ratio of the fuel cell cathode at their nominal values, acting on the converter duty cycle D and the compressor voltage v_{cm} . The problem can be solved with a decoupled control architecture shown in Figure 2. The air flow controller is designed to regulate the oxygen ratio λ_{O_2} feeding back the compressor air flow rate and acting on the compressor voltage. This controller can reach high performance if the stack current is constant or changes slowly. Then, a second controller, working on the converter, optimally regulates the battery state of charge guaranteeing at the same time the requested power (or current to the load) and avoiding the fast transient of the stack current. In particular, it commands the battery to compensate for the power request during the fast transients while using the fuel cell to furnish the desired power and recover the state of charge.

In the following subsections the controllers are described in details.

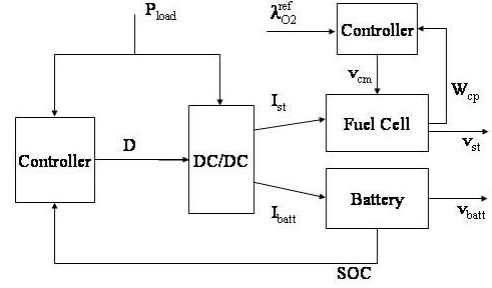


Fig. 2. Decoupled control scheme. Some connections are omitted for sake of readability.

A. Fuel cell operating point regulation

The key features in fuel cell control is the regulation of the oxygen ratio at cathode in order to prevent the oxygen starvation and, as consequence, the performance and the potential life reduction [15], [16]. The main problem is that λ_{O_2} is not measurable but we can estimate it by measuring W_{cp} and inverting equation (3), that approximates the relationship between λ_{O_2} and W_{cp} at steady state. Unfortunately, during the current transients, the error introduced by this approximation propagates to the regulation of the oxygen ratio, causing an inevitable performance reduction. Hence it is critical that the stack current is constant or varies slowly, which will be guaranteed with the DC/DC converter controller.

Here, the adopted control strategy is obtained combining a feedback and feedforward action, as shown in Figure 3. The first is realized via a PI controller, whose input is the error between the measure of W_{cp} and reference W_{cp}^{ref} . This function of the actual stack current is computed by (3) where the oxygen ratio is substituted with its reference value $\lambda_{O_2}^{ref} = 2$.

The feedforward controller is a static function relating the compressor voltage to the stack current at optimal oxygen ratio. This function has been calculated by linearization, approximating the state equations with first order Taylor series. The result, according to

$$v_{cm}^{FF} = 20.16 + 0.712I_{st}, \quad (9)$$

was confirmed by using the full non linear simulation.

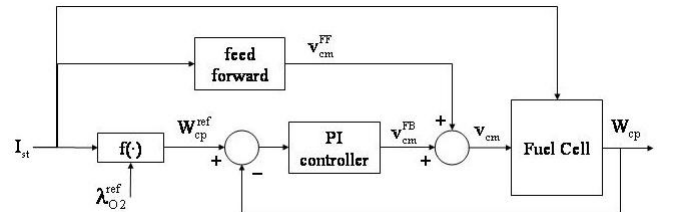


Fig. 3. Fuel cell control scheme

B. Power management

The main component of the proposed architecture is the controller devoted to balance the requested power between

the fuel cell and the battery. The objectives are to regulate the optimal state of charge and minimize the rate of variation of the stack current, subject to the constraint on power demand $P_{load} = v_{batt}I_{load}$. The main idea is to furnish the total load current through the fuel cell at steady state, and to compensate with the battery during the fast transients.

To this aim, we propose an LQ based control strategy designed on the DC/DC converter and battery (see Figure 4), whose equations (4)-(8) are rewritten as

$$\dot{I}_{conv} = -\frac{1}{L}v_{batt}(SOC) + \frac{1}{L}v_{st}(t)D \quad (10a)$$

$$\dot{SOC} = \frac{I_{conv}}{Q_{max}} - \frac{1}{Q_{max}} \frac{P_{load}(t)}{v_{batt}(SOC)} \quad (10b)$$

where I_{conv} and SOC form the state vector x , D is the control input u , and $v_{st}(t)$ and $P_{load}(t)$ are considered as time varying parameters.

The objective function has been selected after taking into account the goals both on the battery state of charge and on the rate of variation of stack current, as follows

$$V = \frac{1}{2} \int_0^{\infty} [(x - \bar{x})^T Q (x - \bar{x}) + \rho(u - \bar{u})^2] dt \quad (11)$$

where (\bar{x}, \bar{u}) is the equilibrium point of system (10) related to the desired SOC value, i.e. $\bar{x}_2 = \overline{SOC} = 80\%$ and

$$\bar{x}_1 = \bar{I}_{conv} = \frac{P_{load}}{\bar{v}_{batt}} \quad (12a)$$

$$\bar{u} = \bar{D} = \frac{\bar{v}_{batt}}{v_{st}} \quad (12b)$$

where \bar{x}_1 and $\bar{v}_{batt} = 10.39$ V the converter current and the battery voltage corresponding to \overline{SOC} .

We have to highlight that we do not consider a battery state of charge estimator (see as an example [3]) but we assume it is known or accurately estimated, since it is out of the scope of the paper.

In order to apply the well known optimal LQ controller, the system (10) is linearized around the equilibrium point (12)

$$\delta \dot{x} = A(t)\delta x + B(t)\delta u \quad (13)$$

where $\delta x = x - \bar{x}$ and $\delta u = u - \bar{u}$ are respectively the deviation of the state and the control input from the equilibrium point, and the time varying matrices $A(t)$ and $B(t)$ are computed according to

$$A(t) = \begin{pmatrix} 0 & -\frac{1}{L} \frac{\partial \bar{v}_{batt}}{\partial SOC} \\ \frac{1}{Q_{max}} & \frac{P_{load}(t)}{Q_{max} \bar{v}_{batt}^2} \frac{\partial \bar{v}_{batt}}{\partial SOC} \end{pmatrix} \quad (14a)$$

$$B(t) = \begin{pmatrix} \frac{v_{st}(t)}{L} \\ 0 \end{pmatrix} \quad (14b)$$

with $\frac{\partial \bar{v}_{batt}}{\partial SOC}$ the change of battery voltage with respect to the SOC evaluated at the nominal \overline{SOC} .

Hence, the objective function (11) is related to the linearized system as follows

$$V = \frac{1}{2} \int_0^{\infty} [\delta x^T Q \delta x + R \delta u^2] dt. \quad (15)$$

The values of the matrix Q and R were determined using the Matlab/Simulink ‘‘Genetic Algorithm and Direct Search Toolbox’’ [1]. The quality index was the quadratic error on λ_{O_2} during a step from 30 kW to 35 kW in requested power and the population size was set to 20. The power split goal allows the management strategy to relax the regulation of the SOC during the most fuel cell stressful manoeuvres, which translates to a larger value for R than Q . The optimal values we found are $Q = \text{diag}(10, 0.143)$ and $R = 10^6$. The control law is

$$\delta u^* = -R^{-1}B(t)^T P \delta x \quad (16)$$

where P is the solution of the Riccati equation. As usual, to avoid an excessive computational cost and to permit an on-line implementation, the suboptimal solution was adopted, obtained by solving the algebraic Riccati equation [2]

$$P(t)A(t) + A(t)^T P(t) - P(t)B(t)R^{-1}B(t)^T P(t) + Q = 0. \quad (17)$$

Finally, the control input can be obtained

$$u^* = \bar{u} - R^{-1}B(t)^T P(x - \bar{x}). \quad (18)$$

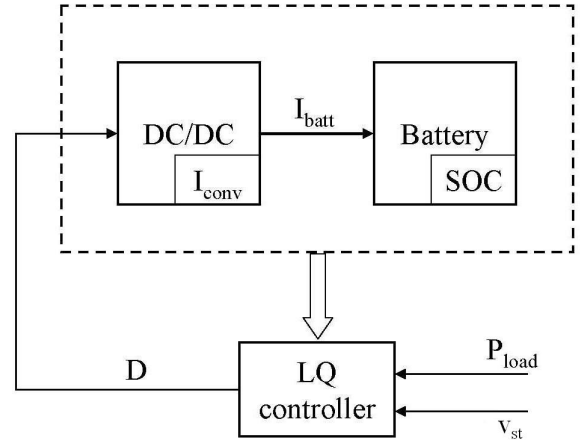


Fig. 4. Power management control. Schematic diagram of the lees.

IV. SIMULATION RESULTS

The performance of the proposed control strategy has been investigated through Matlab/Simulink and real-time simulations. In order to reduce the computational effort during the Matlab/Simulink simulation, the Riccati matrix P was considered constant until the coefficients of the (17), i.e. the matrices A and B , change significantly. These matrices are function of $P_{load}(t)$ and $v_{st}(t)$, so two dynamic threshold were set and the values of the Riccati matrix P was updated when the variation of power request or stack voltage was greater then 1%. Conversely, for HIL simulation, a gain scheduling was computed off-line. A grid was determined function of the power request and stack voltage. Specifically the range for v_{st} was chosen between $v_{st} = 1$ V and $v_{st} = 400$ V with a step of 1 V (400 values in total). For P_{load} the interval was fixed between $P_{load} = 10$ kW

and $P_{load} = 55$ kW with a step of 100 W (450 values in total). The whole grid consisted of 18000 points. The Riccati equation solution P was computed for each point. In the two following section the simulation results will be discussed in detail. In particular, the selected results obtained by the HIL simulation show the feasibility and the robustness of the control architecture.

A. SIL Simulation

A large number of simulations was performed to assess the closed loop performance. A selected simulation in Matlab/Simulink environment is used to demonstrate the results. Figure 5 shows the selected load profile, which is comprised of steps in power demand. In particular during the first 1000 s the power demand exhibits 5 steps starting from a minimum value of 20 kW until a maximum value of 45 kW. During the last 1500 s a constant value (30 kW) was set for the power request in order to evaluate the performance of the strategy in recharging the battery from 50% of the total capacity to the desired SOC value ($SOC = 80\%$). Figures 6-9 summarize the simulation results. The first plot of Figure 6 shows that the oxygen ratio reaches accurately the desired value at steady state, and that the error quickly recovers during the fast power transient. The error on λ_{O_2} is mainly due to the approximation error associated with (3) during stack current transients, that propagates to the oxygen ratio regulation. This argument is confirmed by the second plot of Figure 8, that shows the performance of the controller aimed at the regulation of the compressor air flow rate. This control difficulty could be mitigated by a λ_{O_2} observer. This is a topic that we are now investigating. Nevertheless we want to highlight that a correct power split can support the action of the fuel cell controller in regulating the oxygen ratio and avoid an excessive complexity.

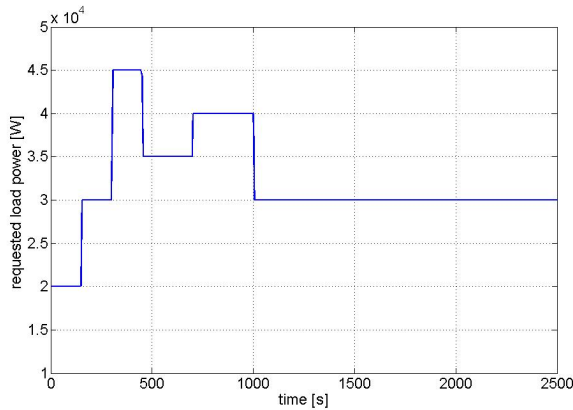


Fig. 5. SIL simulation: requested load power.

Figure 7 shows the performance of the power split strategy, namely the regulation of the battery state of charge and the balancing of the power demand between the two sources. The response of Figure 7 also allows the evaluation of the steady-state closed loop performance, showing that the fuel cell furnish both the desired power and, mainly at the beginning,

the extra power necessary to charge the battery. Indeed, the second plot of Figure 6 shows that the SOC reaches the desired value. Conversely, during the fast transients, the controller compensates with the battery the amount of power that the fuel cell can not provide to not degraded its performance. The first plot of Figure 8 shows how the controller filters the steps in the power demand allowing a smoother fuel cell current behavior. Finally, Figure 9 shows the stack voltage. In conclusion, the simulations demonstrate a good behavior of the controlled system. The controller achieves good balancing between the fuel cell and the battery energy supply aimed at providing the power request and at reaching the nominal operating point.

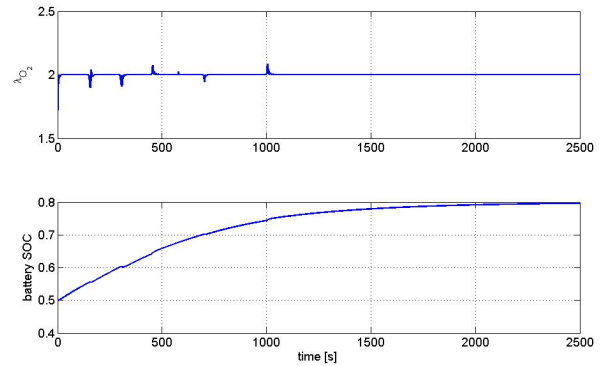


Fig. 6. SIL simulation: battery state of charge and oxygen ratio at cathode.

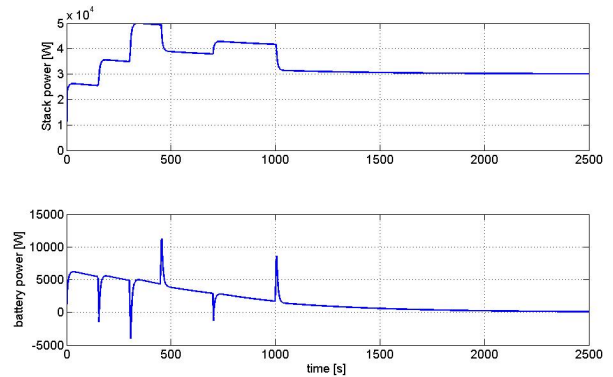


Fig. 7. SIL simulation: fuel cell and battery power flow.

B. HIL Simulation

Real-time experiments have been realized connecting a dSpace MicroAutoBox Electronic Control Unit (ECU) with a dSPACE HIL Simulator Mid-Size through a DS2202 I/O board. The MicroAutoBox processor is a IBM PPC 750FX 800 MHz with a total memory of 28 MB, subdivided in main memory, memory for communication with PC and nonvolatile flash memory. The processor of the dSPACE HIL Simulator Mid-Size is based on a DS1005 processor board

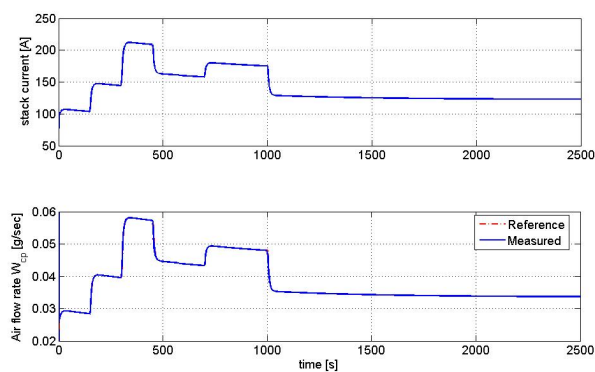


Fig. 8. SIL simulation: stack current and compressor air flow rate.

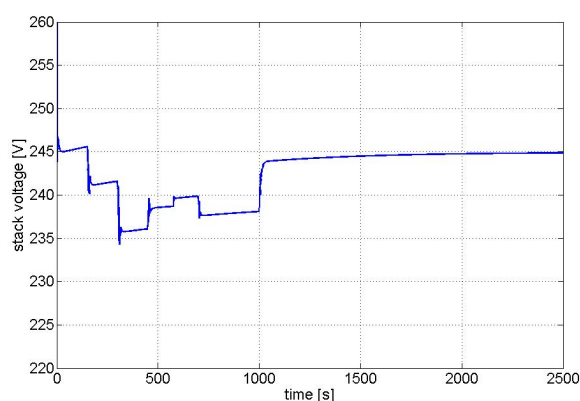


Fig. 9. SIL simulation: stack voltage value.

running at 1 GHz and the I/O board has 20 D/A channels and 16 A/D channels, 38 digital inputs and supports 2-voltage systems. The dSPACE Simulator reproduced the FCHPS model behavior while the control strategy was downloaded in the ECU. The experimental set-up is shown in Figure 10. The closed loop HIL simulation associated with the load profile shown in Figure 11 is discussed below. Again, the power request values range from 20 kW and 50 kW. This power demand was entered manually on-line during the simulation, except for the step from 35 kW to 40 kW that was preprogrammed in the ECU. As consequence, the manual demand steps are not smooth, as the zoom-in in the Figure 11 highlights. Figures 12-15 show the simulation test results. The instantaneous step during the 1000th second demonstrates that the closed loop performance is consistent with the SIL simulation results. The zoom-in at 1000 s in the first plot of Figure 12 shows that the error on the oxygen ratio is less than 1%. Also the stack current (first plot of Figure 13) and the power split (shown in Figure 14) exhibit the expected behavior. The battery very quickly supplies the increasing in the power demand allowing the fuel cell current to change slowly. On the other hand, during the manual demanded steps, the oxygen ratio exhibits a larger error, but it is still less than 5%. The increased oscillation are, mainly, due to

the irregularity in the power request profile. The zoom-in at 1500 s in Figures 13 and 14 show that these irregularities also affect the stack current and the battery power behavior. Despite of these irregularities, the control strategy achieves its main goal as confirmed by the Figure 15, that shows how the requested power and the power supplied by the system perfectly match, highlighting the achieved high performance of the hybrid system in the load following task.

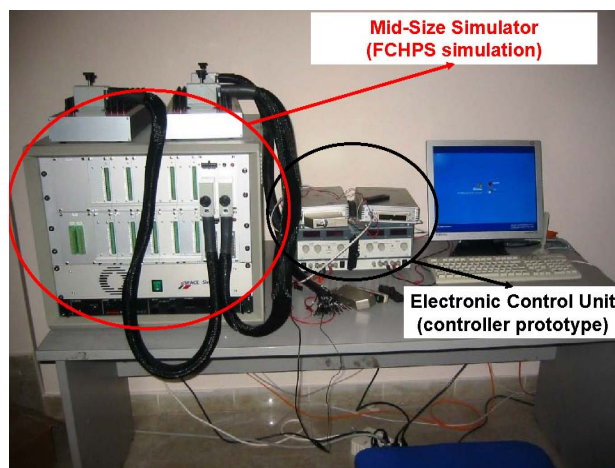


Fig. 10. Experimental set-up.

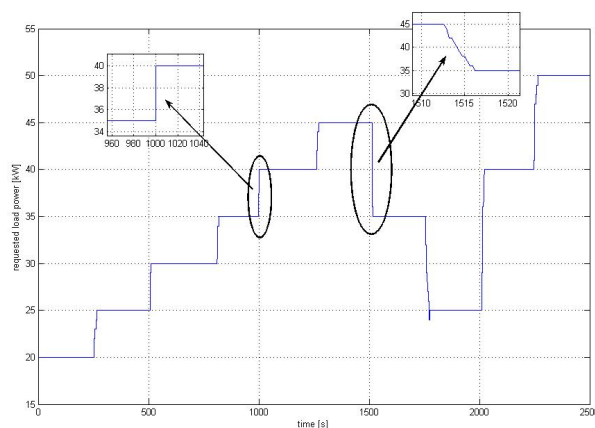


Fig. 11. HIL simulation: request load power.

V. CONCLUSION

The fuel cell performance can be considerable improved with a hybrid configuration which combines a battery through a DC/DC converter. This paper shows a simple decoupled control strategy which allows a good compromise between high performance and safe use of the stack. Here, the fuel cell stack is controlled via a feedforward action and a PI regulator whereas, the DC/DC converter optimizes the current split via a linear quadratic controller.

Good closed loop performance is shown in the Hardware-in-the-Loop experiments. In future work we intend to extend this control strategy after taking into account more realistic

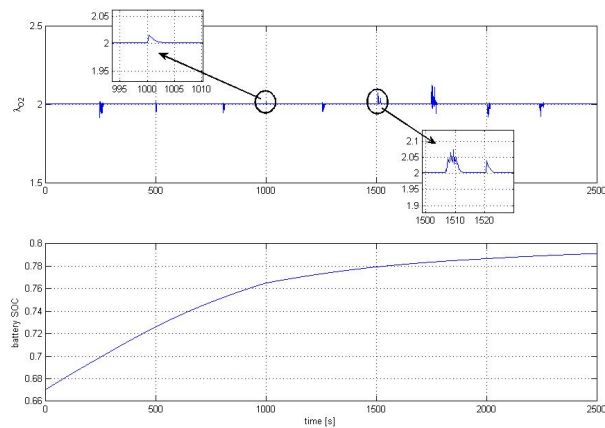


Fig. 12. HIL simulation: oxygen ratio at cathode and battery state of charge.

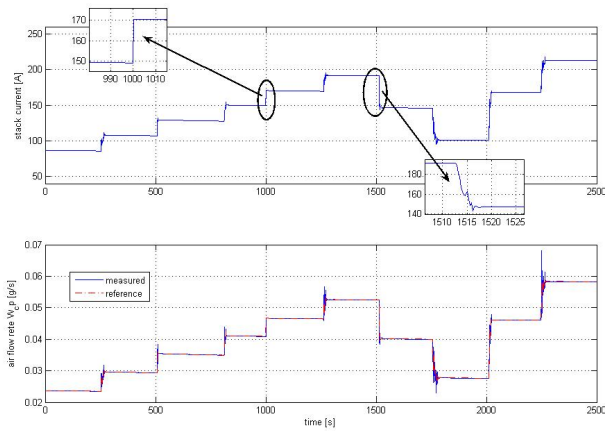


Fig. 13. HIL simulation: stack current and compressor air flow rate.

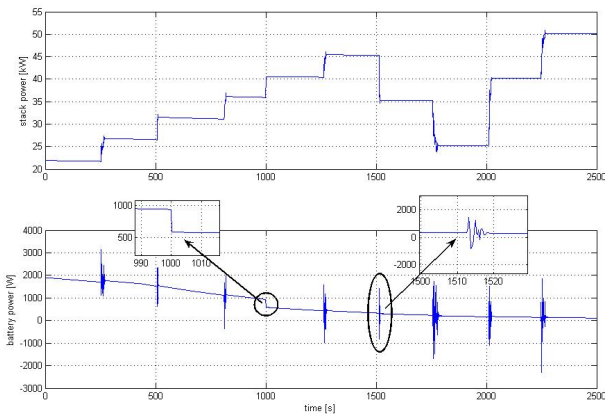


Fig. 14. HIL simulation: fuel cell and battery power flow.

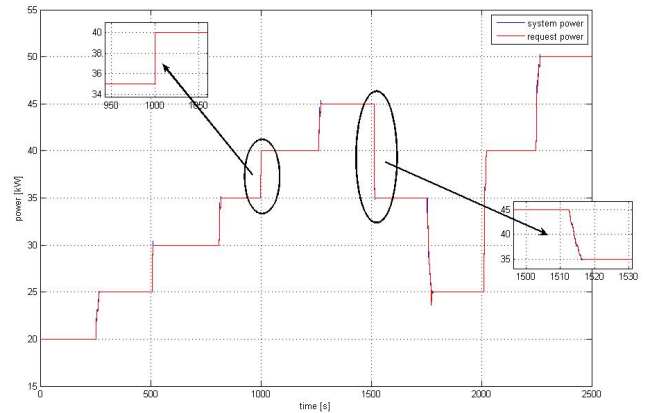


Fig. 15. HIL simulation: request power vs system supplied power.

constraints in the battery power response, include *SOC* estimation and insert in the control loop an observer for the oxygen ratio at cathode.

VI. ACKNOWLEDGMENTS

The authors gratefully acknowledge Francesco Vasca for the helpful discussions and Anna Stefanopoulou for her invaluable suggestions.

REFERENCES

- [1] *Genetic Algorithm and Direct Search Toolbox 2 - Users Guide*. Mathworks, 2005.
- [2] B.D.O. Anderson and J.B. Moore. *Optimal Control: Linear Quadratic Methods*. Prentice Hall, 1990.
- [3] O. Barbarisi, L. Glielmo, and F. Vasca. State of charge kalman filter estimator for automotive batteries. *Control Engineering Practice*, 14:267–275, 2006.
- [4] W. Gao. Performance comparison of a fuel cell-battery hybrid powertrain and a fuel cell-ultracapacitor hybrid powertrain. *IEEE Transactions on Vehicular Technology*, 54:846 – 855, 2005.
- [5] Y. Guezennec, T.-Y. Choi, G. Paganelli, and G. Rizzoni. Supervisory control of fuel cell vehicles and its link to overall system efficiency and low-level control requirements. *American Control Conference*, 3:2055 – 2061, 2003.
- [6] Soo-Bin Han, Suk-In Park, Hak-Geun Jeoung, Bong-Man Jeoung, and Se-Wan Choi. Fuel cell-battery system modeling and system interface construction. *The 29th Annual Conference of the IEEE Industrial Electronics Society*, 3:2623 – 2627, 2003.
- [7] K. Holland, M. Shen, and F.Z. Peng. Z-source inverter control for traction drive of fuel cell-battery hybrid vehicles. *Industry Applications Conference, IAS Annual Meeting*, 3:1651 – 1656, 2005.
- [8] Z. Jiang, L. Gao, and R.A. Dougal. Flexible multiobjective control of power converter in active hybrid fuel cell/battery power sources. *IEEE Transactions on Power Electronics*, 20:244 – 253, 2005.
- [9] A. Nasiri, V.S. Rimmalapudi, A. Emadi, D.J. Chmielewski, and S. Al-Hallaj. Active control of a hybrid fuel cell-battery system. *The 4th International Power Electronics and Motion Control Conference*, 2:491 – 496, 2004.
- [10] J.T. Pukrushpan, H. Peng, and A.G. Stefanopoulou. Control-oriented modeling and analysis for automotive fuel cell system. *Journal of Dynamic Systems, Measurement, and Control*, 126:14–25, 2004.
- [11] J.T. Pukrushpan, A.G. Stefanopoulou, and H. Peng. *Control of Fuel Cell Power Systems: Principles; Modeling; Analysis and Feedback Design*. Springer, 2005.
- [12] K. Rajashekara. Hybrid fuel-cell strategies for clean power generation. *IEEE Transactions on Industry Applications*, 41:682 – 689, 2005.
- [13] A.G. Stefanopoulou. Mechatronics in fuel cell sysetems. *Symposium in Mechatronics*, 2004.

- [14] K.-W. Suh and A.G. Stefanopoulou. Control and coordination of air compressor and voltage converter in load-following fuel cell. *International Journal of Energy Research*, 29:1167–1189, 2005.
- [15] J. Sun and I.V. Kolmanovsky. Load governor for fuel cell oxygen starvation protection: A robust nonlinear reference governor approach. *IEEE Transactions on Control Systems Technology*, 13:911 – 920, 2005.
- [16] A. Vahidi, A.G. Stefanopoulou, and H. Peng. Current management in a hybrid fuel cell power system: A model predictive control approach. *IEEE Transactions Control System Technology*, 14:1047 – 1057, 2004.